Modulation Scheme for Improved Operation of a RB-IGBT Based Resonant Inverter Applied to Domestic Induction Heating

Abstract- **Domestic induction appliances require power converters that feature high efficiency and accurate power control in a wide range of operating conditions. To achieve this aim, modulation techniques play a key role to optimize the power converter operation.**

In this paper, a series resonant inverter featuring reverse blocking IGBTs and an optimized modulation technique are proposed. An analytical study of the converter operation is performed, and the main simulation results are shown. The proposed topology reduces both conduction and switching losses, increasing significantly the power converter efficiency. Besides, the proposed modulation technique achieves linear output power control, improving the final appliance performance. The results derived from this analysis are tested by means of an experimental prototype, verifying the feasibility of the proposed converter and modulation technique.

I. Introduction

Induction heating has been successfully applied to domestic applications due to advantages such as efficiency, fast heating, and safety [1]. The basic structure of an induction heating appliance can be seen in Fig. 1(a). It consist of the power electronics converter, the control electronics, and the inductor-pot system. The power conversion scheme applied to the induction appliance is summarized in Fig. 1(b). The mains voltage is rectified and filtered, generating a DC bus. Afterwards, a dc-ac converter, i.e. inverter, supplies variable frequency current (15 to 75 kHz) to the induction coil. This current produces an alternating magnetic field, which causes eddy currents and magnetic hysteresis heating up the pan.

The inverter is the main block of the induction heating appliance. Different topologies have been proposed as the series resonant half-bridge [2-5], the series resonant full-bridge [6], [7], or the Marx inverter [8], [9]. The election among these topologies depends mainly on the balance between cost and performance for a specific purpose.

The main desired features when designing an inverter for domestic induction heating are the output power control and the efficiency. On one hand, the appliance must operate under a wide range of output power set-points selected by the user, leading to a variety of operating conditions. On the other hand, the efficiency determines not only the environmental impact and the reliability of the appliance, but also the final performance considering the limited possibilities of cooling.

Modulation strategies play a key role to achieve the aforementioned aims. In the past, several modulation techniques have been proposed to optimize either the output power control or the efficiency. In [7], [10], asymmetrical voltage cancelation is proposed to improve efficiency in full-bridge topologies. This modulation scheme is extended to the half-bridge topology through the variable frequency duty cycle control proposed in [11] to optimize the efficiency. In [2], [6], [12], pulse density modulation (PDM) is also proposed to optimize the efficiency in the low-medium output power range. Finally, in [13], [14] discontinuous-mode based modulations are proposed as an alternative to PDM that eliminates flicker emissions and issues related to pulsed power delivered to the induction load. Most of the aforementioned modulation techniques operate above the resonant frequency to obtain a zero voltage switching transition and, consequently, reduce the switching losses.

The aim of this paper is therefore to propose a modulation technique to improve the output power control and efficiency of a resonant inverter applied to domestic induction heating. The inverter topology is a variation of the series resonant half-bridge, featuring reverse-blocking insulated gate bipolar transistors (RB-IGBTs). RB-IGBTs allows to block negative voltage with improved performance when compared to adding a series diode [15-

(a)

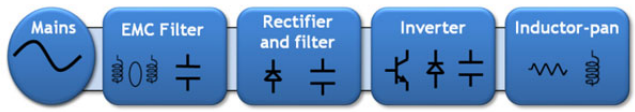

(b)

Fig. 1. Domestic induction heating appliance: general architecture (a) and power conversion scheme (b).

17], and have been proposed for several industrial applications [18-20]. RB-IGBTs have also been applied to induction heating, either in ac-ac converters [21] or in quasi-resonant inverters [22]. In this paper, RB-IGBTs are used to implement an inverter that allows using an improved modulation technique. The proposed modulation technique achieves linear output power control and improved efficiency compared to previous ones, at no additional cost.

This paper is organized as follows. Section II details the proposed reverse-blocking IGBT based inverter. Section III analyzes the proposed modulation technique, focusing on the output power control and the converter efficiency. Section IV describes the experimental test-bench and the main experimental results to probe the feasibility of the proposed system. Finally, the main conclusions of this paper are drawn in Section V.

II. Resonant Inverter Topology

The proposed power converter topology is based on the series resonant half bridge, which is the topology that achieves the best balance between cost and performance considering the domestic induction heating applications. In this proposal, the IGBTs with antiparallel diode have been replaced by RB-IGBTS, as shown in Fig. 2. This provides additional control features which allow easing the output power control and increasing the efficiency.

The resonant tank of the proposed inverter is a series RLC composed of the equivalent resistor R_{eq} and inductance L_{eq} of the inductor-pot system [23], and the resonant capacitor C_r. The equivalent values of the inductor-pot system, R_{eq}, L_{eq}, change with the geometry, pan materials, temperature, and excitation frequency, making the output power control harder. For this reason, a complete analysis of the output power as a function of these equivalent parameters is provided.

Three different configurations are possible for the proposed converter (Fig. 3). In state I, the bus voltage V_b is applied to the load, whereas in state II the load is shor-circuited, i.e. v_o=0. Finally, in state III both switching devices are deactivated and there is no current.

The classical half-bridge series inverter can be operated in two different modes (Fig. 4): zero voltage switching (ZVS) and zero current switching (ZCS). The former operation mode, ZVS, is characterized by a negative phase-lag between current and voltage. As a consequence, when the switch is activated, the current is conducted by the anti-parallel diode and, consequently, ZVS switch-on transition is achieved, minimizing switching losses. The latter operation mode, ZCS, is characterized by a positive phase lag between current and voltage. Consequently, the switch-on transition is achieved without losses. In both operation modes, part of the current recirculates through the diodes to the bus, increasing the conduction losses to deliver a certain output power.

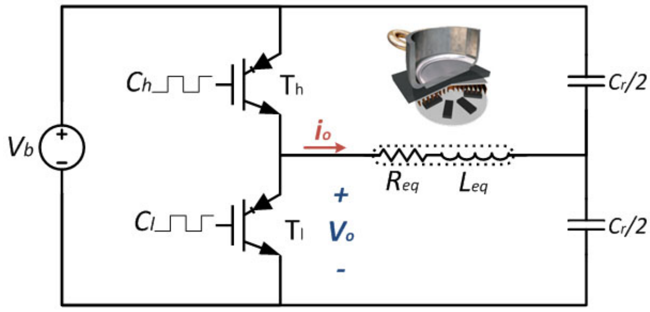

Fig. 2. Proposed converter schematic

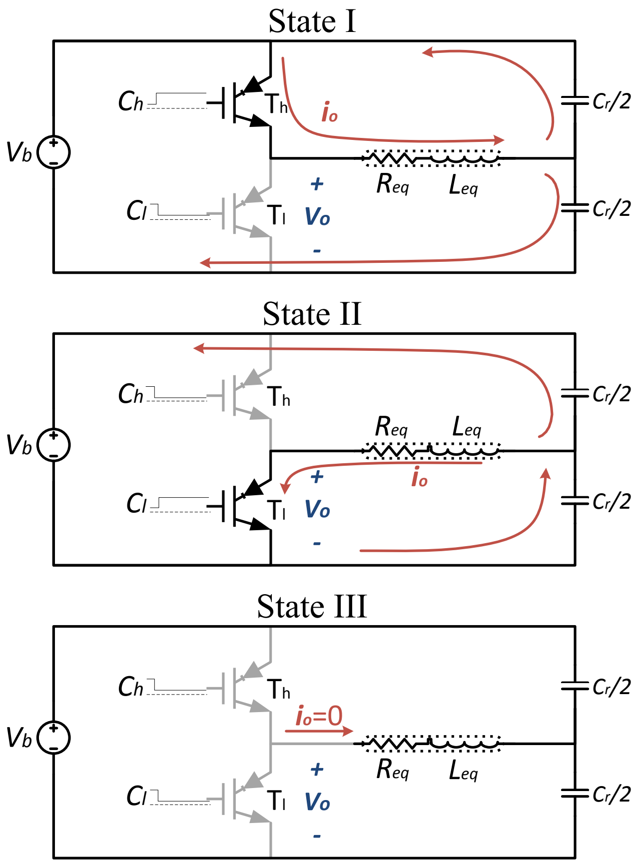

Fig. 3. Equivalent circuit configurations of the proposed series resonant inverter.

The proposed operation mode (Fig. 4) operates at switching frequencies lower than the resonant frequency, as in the ZCS operation mode. However, since there are no antiparallel diodes, once the current extinguishes remains zero until the next switch is activated. At this point, RB-IGBTs are needed to block the negative voltage that may appear due to the voltage of the resonant capacitors. This operation mode achieves ZCS during switch-off transition and negligible switch-on losses due to the fact that the inductor L_{eq} behaves as a high-value inductive snubber. Besides, since no current recirculates to the bus, lower conduction losses are also achieved. A detailed analysis of the power converter operation is presented in the next section.

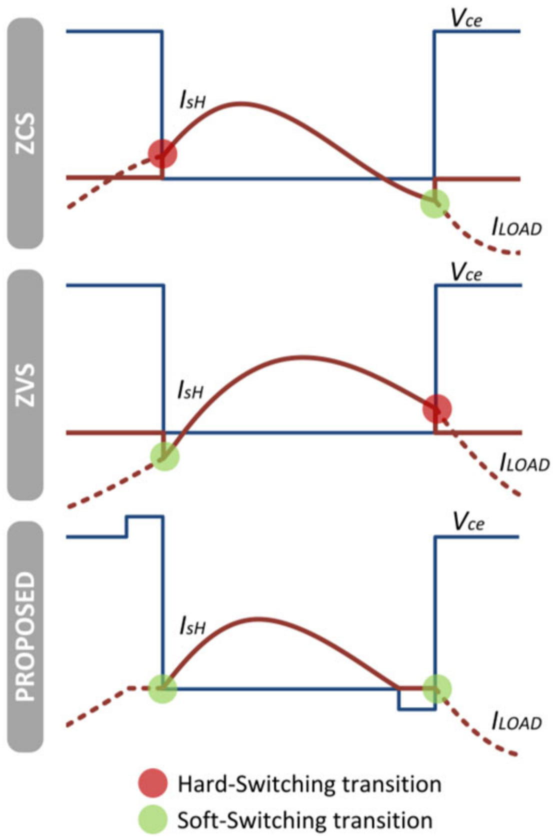

Fig. 4. Operations mode for the half-bridge converter: ZCS and ZVS for the classical half-bridge and the operation mode for the proposed converter.

III. Proposed Modulation Technique

The power converter proposed in this paper offers additional control possibilities to obtain linear output power control with improved efficiency. In this section, a theoretical analysis of the power converter operation is performed. On this basis, an output power control scheme is proposed and the power converter efficiency is analyzed.

A. Theoretical analysis

The converter operation is based on charging and discharging the resonant capacitor through the load in a single current direction. Since the converter presents symmetry, the theoretical analysis is simplified.

Considering the use of RB-IGBTs, i.e. unidirectional devices, the current trough the load stops when it reaches zero. As a result, the resonant capacitor voltage starts from a positive value, higher than the power supply voltage, and ends with a negative value when the current reaches zero.

The differential equation that defines the current trough the load can be obtained by the Kirchhoff's circuit laws:

$$i_o(t)R_{eq} + L_{eq}\frac{di_o(t)}{dt} + \frac{1}{C_r}\int_0^t i_o(\tau)d\tau = 0. \tag{1}$$

Using the Laplace transform, equation (1) can be expressed as a second order lineal equation in the transformed domain s.

$$R_{eq} + sL_{eq} + \frac{1}{sC_r} = 0, \tag{2}$$

that can be rewritten as a second order dynamical system

$$s^2 + \frac{R_{eq}}{L_{eq}}s + \frac{1}{L_{eq}C_r} = 0. \tag{3}$$

Second order dynamical systems can be parameterized as a function of the damping factor ξ and the resonant angular frequency ω_0, defined by:

$$\xi = \frac{R_{eq}}{2L_{eq}}. \tag{4}$$

$$\omega_o = \sqrt{\frac{1}{L_{eq}C_r}}. \tag{5}$$

The dynamic of the second order system must be underdamped in order to achieve zero current switching-off transitions. Consequently, the natural angular frequency ω_n can be defined as:

$$\omega_n = \sqrt{\omega_o^2 - \xi^2}. \tag{6}$$

The roots of the second order linear system in the s-domain are:

$$S_{1,2} = -\xi \pm j\omega_n. \tag{7}$$

Applying the inverse Laplace transform, the temporal domain response for the resonant capacitor voltage v_{C_r} is:

$$v_{C_r}(t) = Be^{-\xi t}\sin(\omega_n t + \beta). \tag{8}$$

Where the freedom parameters $\{B, \beta\}$ can be determined as considering two temporal restrictions: the resonant capacitor voltage at time zero is $v_{C_r}(t=0) = V_{C_r}$; and the derivative of the voltage at time zero is 0. Applying these restrictions to (8), the following expressions are obtained:

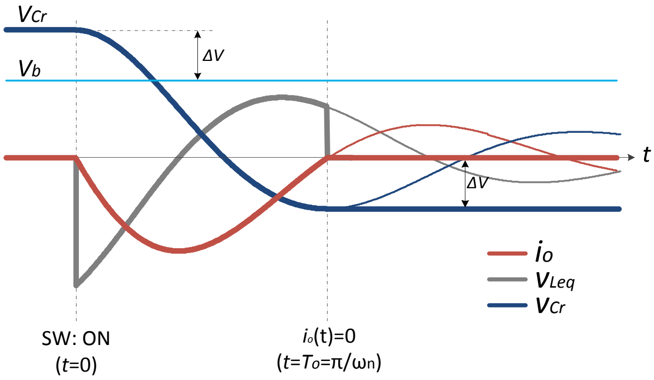

Fig. 5. Main resonant waveforms of the proposed converter using the analytical model presented.

$$\begin{cases} v_{C_r}(t=0)=V_{C_r} \;\Rightarrow\; B\sin(\beta)=V_{C_r} \\ \left.\dfrac{dv_{C_r}(t)}{dt}\right|_{t=0}=0 \;\Rightarrow\; -\xi\sin(\beta)+\omega_n\cos(\beta)=0 \end{cases}. \quad (9)$$

By rewriting these conditions, the freedom parameters can be determined:

$$\begin{cases} B=\dfrac{V_{C_r}}{\sin(\beta)} \;\Rightarrow\; \mathrm{B}=V_{C_r}\dfrac{\omega_o}{\omega_n} \\ \beta=\mathrm{atan}\left(\dfrac{\omega_n}{\xi}\right) \end{cases}. \quad (10)$$

Hence, the time-domain response of the resonant capacitor voltage is:

$$v_{C_r}(t)=V_{C_r}\frac{\omega_o}{\omega_n}e^{-\xi t}\sin(\omega_n t+\beta). \quad (11)$$

Consequently, the load current i_0 and the inductor voltage $v_{L_{eq}}$ are:

$$i_0(t)=C_r\frac{dv_{C_r}(t)}{dt}=\frac{-V_{C_r}}{L_{eq}\omega_n}e^{-\xi t}\sin(\omega_n t), \quad (12)$$

$$v_{L_{eq}}(t)=L_{eq}\frac{di(t)}{dt}=V_{C_r}\frac{\omega_o}{\omega_n}e^{-\xi t}\sin(\omega_n t-\beta). \quad (13)$$

The load current is stopped when it reaches zero, consequently, the resonant period can be defined as T_o:

$$i_0(t>0)=0 \Rightarrow e^{-\xi t}\sin(\omega_n t)=0 \Rightarrow T_o=\frac{\pi}{\omega_n}. \quad (14)$$

All the temporal signals can be shown in Fig. 5 for a half-switching period.

The resonant capacitor voltage starts from a positive value higher than the supply voltage and finish with a negative value. The positive offset from the supply voltage V_b and the negative offset from zero-level is the same and it is defined by ΔV. This voltage-offset can be solved by applying these conditions:

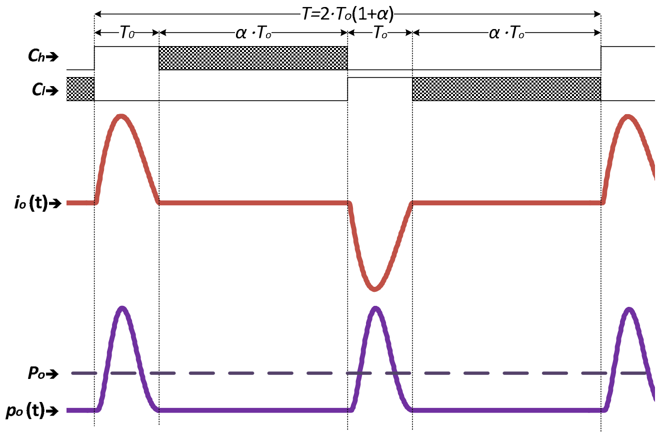

Fig. 6. Proposed modulation scheme and main waveforms (current trough the load and output power).

$$\begin{cases} v_{C_r}(t=0)=V_b+\Delta V=V_{C_r}\dfrac{\omega_o}{\omega_n}\sin(\beta) \\ v_{C_r}(t=T_o)=-\Delta V=V_{C_r}\dfrac{\omega_o}{\omega_n}e^{-T_o\xi}\sin(\pi+\beta) \end{cases}. \quad (15)$$

Hence, the resonant capacitor voltage can be determined by (16), applying $\sin(\beta)=\omega_n/\omega_o$.

$$V_{C_r}=V_b\frac{\omega_n}{\omega_o}\left(\sin(\beta)+e^{-T_o\xi}\sin(\beta+\pi)\right)^{-1}=\frac{V_b}{1-e^{-T_o\xi}}. \quad (16)$$

As a result, the additional voltage offset for the switching devices is:

$$\Delta V=\left(\frac{1}{1-e^{-T_o\xi}}-1\right)V_b. \quad (17)$$

B. *Output power control*

The output power control strategy for the proposed converter is based on the switching frequency variation. The maximum output power is achieved at the resonant frequency and it is reduced as the switching frequency is decreased from the resonant frequency.

As a result, the output power variation is linear with switching frequency and can be calculated using the load current and the equivalent resistor of the inductor-pot system as follows.

$$P = \frac{1}{T}\int_0^T R_{eq} i_o^2(t)dt = 2\left(\frac{1}{T}\int_0^{T_0} R_{eq} i_o^2(t)dt\right). \quad (18)$$

As shown in Fig. 6, the current circulates during two periods T_o in each the switching period T. Two freedoms intervals can therefore be defined, with a length αT_o each one. As a result, the output power can be rewritten as:

$$P_o = \frac{1}{T_o(1+\alpha)}\int_0^{T_o} R_{eq} i_o^2(t)dt. \quad (19)$$

Applying the load current equation (12) in this expression, it is obtained that:

$$P_o = \frac{R_{eq} V_{C_r}^2}{4T_o(1+\alpha)\xi(\omega_n^2+\xi^2)L_{eq}^2}\left(1-e^{-2T_o\xi}\right). \quad (20)$$

This equation can be rewritten using the resonant capacitor voltage, leading to:

$$P_o = \frac{1}{T_o(1+\alpha)}\frac{V_b^2}{2\omega_o^2 L_{eq}}\frac{\left(1-e^{-2T_o\xi}\right)}{\left(1-e^{-T_o\xi}\right)^2}. \quad (21)$$

Finally, the output power can be expressed as:

$$P_o = \frac{1}{(1+\alpha)}P_{o,\max}, \quad (22)$$

where $P_{o,max}$ is:

$$P_{o,\max} = \frac{V_b^2}{2T_o\omega_o^2 L_{eq}}\frac{\left(1-e^{-2T_o\xi}\right)}{\left(1-e^{-T_o\xi}\right)^2}. \quad (23)$$

In (22), it can be seen that the output power varies linearly with $1/1+\alpha$, making the output power control easier than in classical ZVS modulation schemes. Besides, unlike ZVS modulation schemes, the proposed control reduces the switching frequency in order to reduce the output power. As a consequence, the efficiency in the low-medium output power range is not compromised due to the high switching frequencies.

Finally, when designing the modulation scheme, it must be also considered that some temporal restrictions must be taken into account. Firstly, and according to Fig. 6, $T \geq 2T_o$, which means that the converter must operate under the resonant frequency of the load. Otherwise, ZVS operation would be achieved. Secondly, the switching frequency must be high enough to avoid audible noise, which is usually issued in the 20 Hz to 15 kHz range.

C. Efficiency analysis

The power losses of the proposed converter can be divided into conduction losses and switching losses. Switching losses can also be classified in switch-on and switch-off losses. Firstly, the turn-on process is done without losses because the parasitic capacitance of the RB-IGBT can be neglected at the switching frequency, and the inductor-pot system acts as an inductive snubber. Secondly, the turn-off switching losses can be also neglected due to the low reverse recovery time of the devices in the converter operating conditions.

Conduction losses are therefore the main losses for the proposed converter and modulation scheme. Assuming a R_{on}-V_{on} model [11] for the RB-IGBT, conduction losses can be calculated as a function of the mean and the root mean square current through the load as follows:

$$P_{losses} = 2\left(I_{sw,avg}V_{on} + I_{sw-rms}^2 R_{on}\right), \quad (24)$$

where V_{on} and R_{on} are the saturation collector-to-emitter voltage and the conducting resistance of the switching devices, respectively. The mean and rms current can be calculated using these equations:

$$\begin{aligned} I_{sw,avg} &= \frac{1}{T}\int_0^T i_o(t)dt = \frac{1}{T}\int_0^{T_o}\frac{V_{Cr}}{L_{eq}\omega_n}e^{-\xi t}\sin(\omega_n t)dt = \\ &= \frac{V_{Cr}}{TL_{eq}\omega_o^2}\left(1+e^{-\xi T_o}\right) = \frac{V_b}{TL_{eq}\omega_o^2}\left(\frac{1+e^{-\xi T_o}}{1-e^{-\xi T_o}}\right) = \\ &= \frac{1}{1+\alpha}\frac{V_b}{2T_o L_{eq}\omega_o^2}\left(\frac{1+e^{-\xi T_o}}{1-e^{-\xi T_o}}\right) = \frac{1}{1+\alpha}K_{I,avg}, \end{aligned} \quad (25)$$

where $K_{I,avg}$ is:

$$K_{I,avg} = \frac{V_b}{2T_o L_{eq}\omega_o^2}\left(\frac{1+e^{-\xi T_o}}{1-e^{-\xi T_o}}\right). \quad (26)$$

Besides, the rms current is:

$$\begin{aligned} I_{rms} &= \sqrt{\frac{1}{T}\int_0^T i_o^2(t)dt} = \sqrt{\frac{1}{T}\int_0^{T_o}\left(\frac{V_{Cr}}{L_{eq}\omega_n}\right)^2 e^{-2\xi t}\sin^2(\omega_n t)dt} = \\ &= \frac{V_{Cr}}{\sqrt{T}L_{eq}\omega_n}\sqrt{\int_0^{T_o} e^{-2\xi t}\sin^2(\omega_n t)dt} = \\ &= \frac{V_{Cr}}{\sqrt{T}L_{eq}2\sqrt{\xi}\omega_o}\sqrt{1-e^{-2\xi T_o}} = \\ &= \sqrt{\frac{1}{1+\alpha}}\frac{V_b}{\sqrt{8\xi T_o}L_{eq}\omega_o}\frac{\sqrt{1-e^{-2\xi T_o}}}{1-e^{-\xi T_o}} = \sqrt{\frac{1}{1+\alpha}}K_{I,rms}, \end{aligned} \quad (27)$$

where the $K_{I,rms}$ is:

Table I
Proposed inverter specifications

Parameter	Value
f_{s_min}	15 kHz
f_{s_max}	40 kHz
C_r	180 nF
R_{eq}	14.2 Ω
L_{eq}	64 μH
RB-IGBTs	IXRP 15N120

$$K_{1,rms} = \frac{V_b}{\sqrt{8\xi T_o} L_{eq} \omega_o} \frac{\sqrt{1-e^{-2\xi T_o}}}{1-e^{-\xi T_o}}. \tag{28}$$

Consequently, the efficiency as a function of the control parameter can be analyzed, leading to:

$$\eta(\alpha) = (P_o - P_{losses}) / P_o = \\ = \frac{\frac{1}{1+\alpha} P_{o,\max} - \left(\frac{1}{1+\alpha} K_{1,avg} V_{on} + \left(\sqrt{\frac{1}{1+\alpha}} K_{1,avg} \right)^2 R_{on} \right)}{\frac{1}{1+\alpha} P_{o,\max}} = \\ = \frac{P_{o,\max} - \left(K_{1,avg} V_{on} + R_{on} K_{1,rms}^2 \right)}{P_{o,\max}}. \tag{29}$$

From this expression can be seen that the output power and the losses vary in the same amount, and consequently, the efficiency remains constantly for any value of $P_o(\alpha)$.

IV. Experimental Results

An experimental prototype has been designed and built to verify the analytical results previously presented. The system has been designed to supply an induction heating load up to 1 kW. The inductor-pot system is modeled as a series resistor R_{eq} = 14.2 Ω and inductance L_{eq} = 64 μH. The switching frequency limits have been set to 15 kHz to avoid acoustic noise, and lower than resonant frequency to operate in the appropriate operation mode.

The converter is controlled by a control architecture composed of a microcontroller and an ASIC [24], [25]. The microcontroller establishes the modulation parameters, whereas the ASIC generates the gating signals for the RB-IGBTs. The main converter specifications are summarized in Table I.

The main inverter waveforms are shown in Fig. 7 for different output power levels from 500 to 1200 W. The power converter behaves as expected, verifying the analytical results. It should be noted that the waveforms of load current have an offset due to the Rogowsky coil used in the experimentation.

Fig. 9 shows the output power curve as a function of the switching frequency. As it has been explained before, this converter achieves linear output power control, making easier to manage complex induction heating loads.

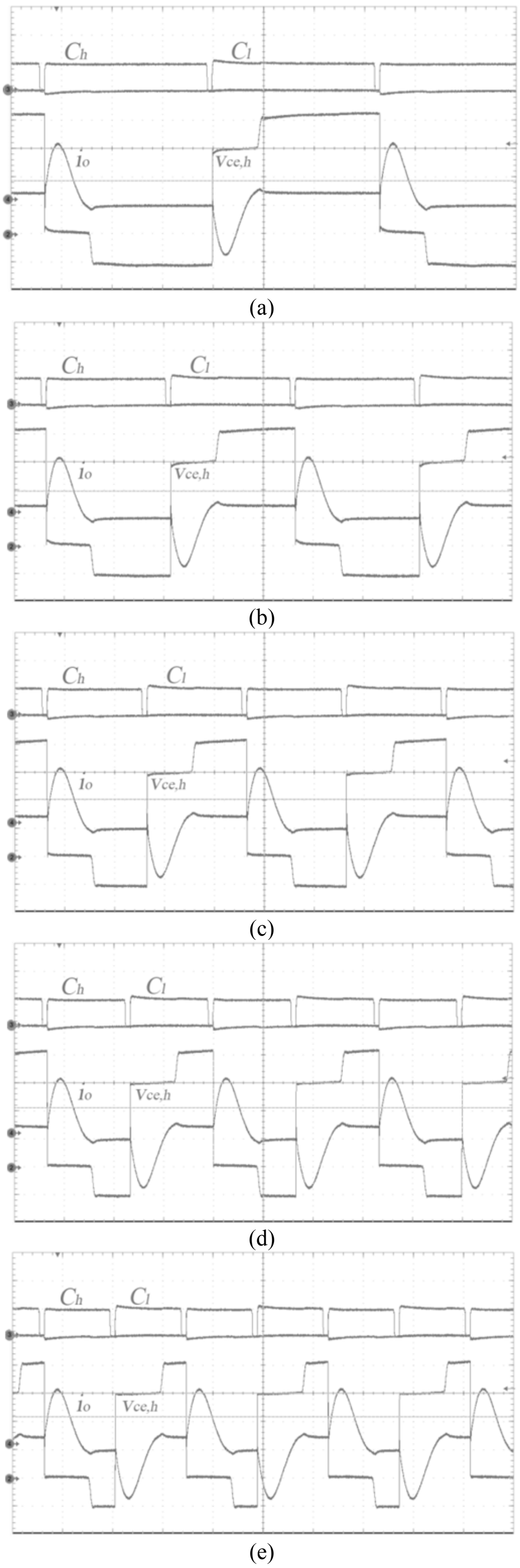

Fig. 7. Main waveforms for the proposed converter for different switching frequencies: 15 kHz for (a), 20 kHz for (b), 25 kHz for (c), 30 kHz for (d) and 35 kHz for (d). Activation signals C_h and C_l (20 V/div), upper switching device voltage $V_{ce,h}$ (100 V/div) and output current i_o (10 A/div). Time: 10 μs/div.

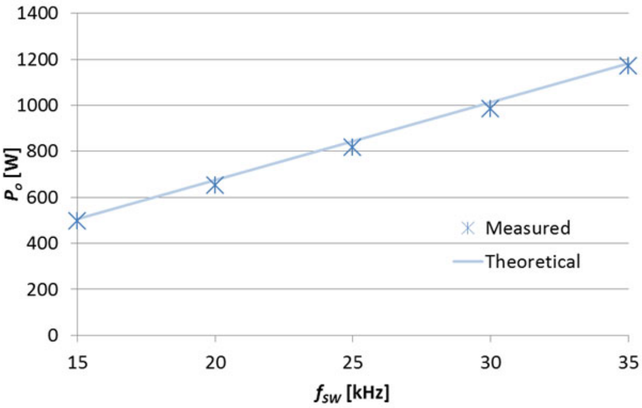

Fig. 9. Theoretical and experimental results for the power converter output power control.

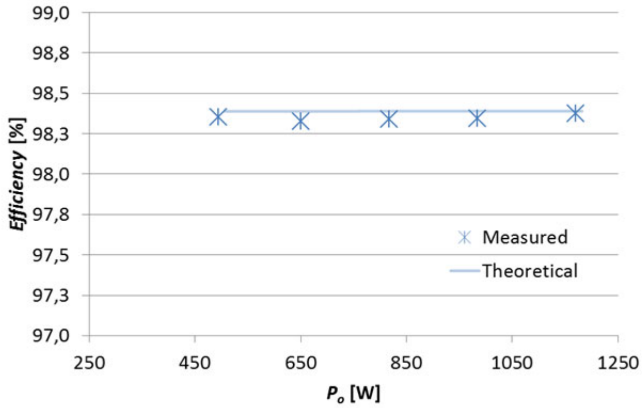

Fig. 8. Efficiency plot for the proposed converter and control strategy.

Finally, an efficiency analysis has been performed to verify the results presented in this paper. The efficiency plot shown in Fig. 8 confirms the flat efficiency curve expected, and probes the proper power converter performance. Besides, it validates the assumption made when neglecting the switching losses.

V. CONCLUSIONS

The efficiency is one of the most important factors of an induction cooker because it not only reduces the energy consumption but also increase the output power reliability. In this paper, a new converter based on the half-bridge topology has been presented. This converter uses the recently developed RB-IGBTs in order to allow using a specific modulation technique.

The power converter operation has been analyzed and the main equations have been derived. A modulation scheme has been proposed taking advantage of the use of RB-IGBTS. This modulation scheme reduces the switching losses and minimizes conduction losses, since the current do not recirculate through free-wheeling diodes to the bus. Besides, the output power can be easily controlled by reducing the switching frequency, avoiding the issues related to high-switching frequencies present in other topologies.

The analytical model presented in this paper has been verified by means an induction heater prototype. Experimental results confirm the feasibility of the proposed converter and modulation scheme. As a conclusion, the improved efficiency and linear output power control makes this topology suitable for the domestic induction heating application.

REFERENCES

[1] J. Acero, et al., "Domestic Induction Appliances," *IEEE Industry Applications Magazine,* vol. 16, no. 2, pp. 39-47, March/April 2010.

[2] O. Lucía, J. M. Burdío, I. Millán, J. Acero, and D. Puyal, "Load-adaptive control algorithm of half-bridge series resonant inverter for domestic induction heating," *IEEE Transactions on Industrial Electronics,* vol. 56, no. 8, pp. 3106-3116, August 2009.

[3] H. Pham, H. Fujita, K. Ozaki, and N. Uchida, "Phase angle control of high-frequency resonant currents in a multiple inverter system for zone-control induction heating," *to be published in IEEE Transactions on Power Electronics,* vol. x, no. x, pp. 1-10, 2011.

[4] H. Fujita, N. Uchida, and K. Ozaki, "A new zone-control induction heating system using multiple inverter units applicable under mutual magnetic coupling conditions," *IEEE Transactions on Power Electronics,* vol. 26, no. 7, pp. 2009-2017, 2010.

[5] B. Saha, K. Soon Kurl, N. A. Ahmed, H. Omori, and M. Nakaoka, "Commercial frequency AC to high frequency AC converter with boost-active clamp bridge single stage ZVS-PWM inverter," *IEEE Transactions on Power Electronics,* vol. 23, no. 1, pp. 412-419, January 2008.

[6] V. Esteve, et al., "Improving the efficiency of IGBT series-resonant inverters using pulse density modulation," *IEEE Transactions on Industrial Electronics,* vol. 58, no. 3, pp. 979-987, March 2011.

[7] S. Chudjuarjeen, A. Sangswang, and C. Koompai, "An improved LLC resonant inverter for induction-heating applications with asymmetrical control," *IEEE Transactions on Industrial Electronics,* vol. 58, no. 7, pp. 2915-2925, July 2011.

[8] J. I. Rodriguez and S. B. Leeb, "Nonresonant and resonant frequency-selectable induction-heating targets," *IEEE Transactions on Industrial Electronics,* vol. 57, no. 9, pp. 3095-3108, September 2010.

[9] J. I. Rodriguez and S. B. Leeb, "A multilevel inverter topology for inductively coupled power transfer," *IEEE Transactions on Power Electronics,* vol. 21, no. 6, pp. 1607-1617, 2006.

[10] J. M. Burdío, L. A. Barragán, F. Monterde, D. Navarro, and J. Acero, "Asymmetrical voltage-cancelation control for full-bridge series resonant inverters," *IEEE Transactions on Power Electronics,* vol. 19, no. 2, pp. 461-469, March 2004.

[11] O. Lucía, J. M. Burdío, I. Millán, J. Acero, and L. A. Barragán, "Efficiency oriented design of ZVS half-bridge series resonant inverter with variable frequency duty cycle control," *IEEE Transactions on Power Electronics,* vol. 25, no. 7, pp. 1671-1674, July 2010.

[12] N. A. Ahmed, "High-frequency soft-switching ac conversion circuit with dual-mode PWM/PDM control strategy for high-power IH applications," *IEEE Transactions on Industrial Electronics,* vol. 58, no. 4, pp. 1440-1448, April 2011.

[13] O. Lucía, J. M. Burdío, L. A. Barragán, J. Acero, and C. Carretero, "Series resonant multi-inverter with discontinuous-mode control for improved light-load operation," *IEEE Transactions on Industrial Electronics,* vol. 58, no. 11, pp. 5163-5171, November 2011.

[14] I. Millán, D. Puyal, J. M. Burdío, C. Bemal, and J. Acero, "Improved performance of half-bridge series resonant inverter for induction heating with discontinuous mode control," in *IEEE Applied Power Electronics Conference and Exposition*, 2007, pp. 1293-1298.

[15] M. Vellvehi, J. L. Galvez, X. Perpina, X. Jorda, P. Godignon, and J. Millan, "Trench isolation technique for reverse blocking IGBT using Boron nitride doping wafers," in *13th European Conference on Power Electronics and Applications EPE '09.*, 2009, pp. 1-5.

[16] J. M. Leisten, A. K. Lefedjiev, and L. Hobson, "Single ended resonant power supply for induction heating," *Electronics Letters,* vol. 26, no. 12, pp. 814-816, December 1990.

[17] H. Kifune, Y. Hatanaka, and M. Nakaoka, "Quasi-series-resonant-type soft-switching phase shift modulated inverter," *IEE Proceedings Electric Power Applications,* vol. 150, no. 6, pp. 725-732, June 2003.

[18] L. Gang, S. Kai, H. Lipei, and I. Seiki, "RB-IGBT gate drive circuit and its application in two-stage matrix converter," in *IEEE Applied Power Electronics Conference and Exposition*, 2008, pp. 245-251.

[19] P. J. Grbovi, F. Gruson, N. Idir, and P. Le Moigne, "Turn-on performance of reverse blocking IGBT (RB IGBT) and optimization using advanced gate driver," *IEEE Transactions on Power Electronics,* vol. 25, no. 4, pp. 970-980, May 2010.

[20] S. Kai, D. Zhou, H. Lipei, K. Matsuse, and K. Sasagawa, "A novel commutation method of matrix converter fed induction motor drive using RB-IGBT," *IEEE Transactions on Industry Applications,* vol. 43, no. 3, pp. 777-786, May/June 2007.

[21] H. Sugimura, S.-P. Mun, S.-K. Kwon, T. Mishima, and M. Nakaoka, "High-frequency resonant matrix converter using one-chip reverse blocking igbt-based bidirectional switches for induction heating," in *IEEE Power Electronics Specialists Conference*, 2008.

[22] S. Wang, K. Izaki, I. Hirota, H. Yamashita, H. Omori, and M. Nakaoka, "Induction-heated cooking appliance using new quasi-resonant ZVS-PWM inverter with power factor correction," *IEEE Transactions on Industry Applications,* vol. 34, no. 4, pp. 705-712, July/August 1998.

[23] J. Acero, C. Carretero, I. Millán, O. Lucía, R. Alonso, and J. M. Burdío, "Analysis and modeling of planar concentric windings forming adaptable-diameter burners for induction heating appliances," *IEEE Transactions on Power Electronics,* vol. 26, no. 5, pp. 1546-1558, May 2011.

[24] O. Lucía, L. A. Barragán, J. M. Burdío, O. Jiménez, D. Navarro, and I. Urriza, "A versatile power electronics test-bench architecture applied to domestic induction heating," *IEEE Transactions on Industrial Electronics,* vol. 58, no. 3, pp. 998-1007, March 2011.

[25] E. Monmasson, L. Idkhajine, M. N. Cirstea, I. Bahri, A. Tisan, and M. W. Naouar, "FPGAs in industrial control applications," *IEEE Transactions on Industrial Informatics,* vol. 7, no. 2, pp. 224-243, May 2011.